Chapter 6
The Methods of Radar Detection of Landmarks by Mobile Autonomous Robots

Oleksandr Poliarus and Yevhen Poliakov

Abbreviations

GPS	Global Positioning System
MAR	Mobile autonomous robots
EMW	Electromagnetic waves
AP	Antenna pattern
RCS	Radar cross section

6.1 Introduction

The development of the theory and practice of modern mobile autonomous robots (MAR) involves providing the necessary accuracy of their navigation in unknown terrain of the earth or another planet. The robot's position on the earth surface is qualitatively determined by the GPS or other navigation system, but in some cases, the efficiency of the GPS can be reduced, for example, due to the limited visibility of the satellites. In such situations, it is convenient to use on-board sensors of various types to determine the coordinates of various objects of the environment [1] or important navigating landmarks. These landmarks are used to measure the angular coordinates of a robot and to solve the problem of its localization [2]. The logical approach is to place on-board sensors in different ranges of electromagnetic waves (EMW) (microwave, optical range, etc.). They scan the surrounding space and find obstacles that appear on the way of the robot. Not all objects outside the robot's path may

O. Poliarus (✉) · Y. Poliakov
Kharkiv National Automobile and Highway University, Kharkiv, Ukraine

O. Sergiyenko et al. (eds.), *Machine Vision and Navigation*,
https://doi.org/10.1007/978-3-030-22587-2_6

represent much interest for it, but if some of these objects are clearly distinguished above the ground and have the known coordinates, they are potential landmarks for the robot. If the robot reliably detects them and determines their coordinates with the desired accuracy, then the practical use of landmarks becomes real. As a rule, these landmarks are passive ones, that is, they only reflect the electromagnetic waves generated by the radar transmitter that is located at the robot. Near them, there are many secondary emitters (separate dimensional objects, trees, dense bushes, vegetation, the earth's surface irregularities, etc.) that create the background of reflected signals whose amplitudes may exceed the amplitude of the signal reflected from the landmark. The sounding of the surrounding space by a robot is often performed in the range of light wavelengths [3, 4] or in other bandwidths of the frequencies [5]. The chapter discusses only the radiofrequency range of waves in the interest of detecting landmarks and determining their coordinates. This wavelength range may be basic or additional one depending on the tasks facing the robot. The possibilities of simultaneous use of different wavelength ranges for solving the main objectives of the robot are also discussed in the chapter. In conditions where it is impossible to detect the echo signal from the landmark, a method for detecting the abrupt changes in signal amplitude during the scanning of landmarks of a special form is proposed.

6.2 The Navigation Problem of Mobile Autonomous Robots

Let the mobile autonomous robot navigate in unknown terrain in the absence of GPS signals on it. A radar or several small radars operating at different frequencies, which differ significantly, are mounted on a robot's board. The system can operate together with laser, ultrasound, and other measuring systems and can duplicate the capabilities of the technical vision system. Information from all measurers is processed by the system of intellectual data analysis, which makes the decision on the robot's position on the ground, as well as the type of terrain, the shape of the relief, which is also necessary for navigation. The chapter deals with a comprehensive approach to radio navigation problems and discusses some issues related to the integration of measuring information.

We believe that a robot scans the surrounding space for determining the position of the robot on the terrain, classification of the type of terrain, and the shape of the relief. All surrounding objects are divided into concentrated and distributed ones. The examples of concentrated objects are objects of human activity (cars, pillars, separate buildings), as well as natural ones (a separate tree, a hill in plain terrain). The distributed objects are almost all the continuous buildings in the city, forest, cross-country, etc.). Radio navigation of mobile robots, as a rule, can be done using concentrated objects with known coordinates. If the coordinates of a single object are determined in the process of measurement, then in some cases, this object can be considered as reference one. The distributed objects of a specific form that clearly stood out against a background of the environment can also be used to navigate

the robots. The radar method involves radiation of the objects by EMW of different frequency. Let us consider the top view on the edge of an even surface without vegetation, which is irradiated by a radar of a robot (Fig. 6.1).

Reflected electromagnetic waves are formed on even surfaces, the centers of which are points A, B, C, D, but in the direction toward the radar antenna, the reflected signal (echo signal) comes only from point B. It carries information about the distance from the radar to point B, but for the conditions of Fig. 6.1, this is the distance to the entire surface.

If the flat (in global sense) surface has a small-scale irregularity with mean height h or vegetation (grass, bushes), etc., the reflected signals reach the antenna radar from all points of this surface (Fig. 6.2).

The signal reflected at point B has the greatest amplitude. At the input of the receiver of the radar in the process of scanning, there will be a random process of amplitudes of echo-signals with an abrupt increase of amplitude at the moment of passing the direction of the main lobe of the radar antenna pattern (AP) through this point. Such a sharp increase of random amplitude at a certain point in time is called the "jump" of the amplitude. The analysis of such jumps is carried out further, where the possibility of their application for navigating robots is also estimated.

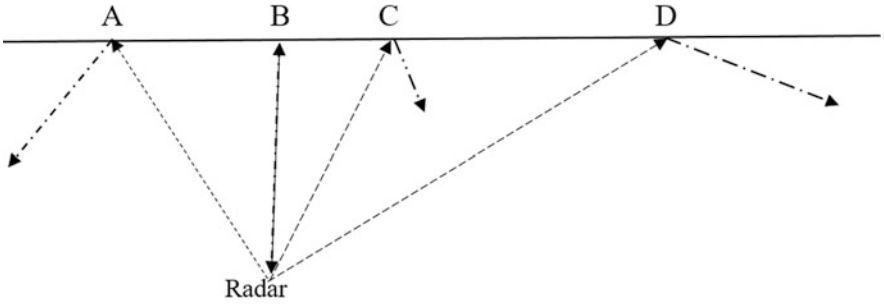

Fig. 6.1 The scheme of reflection signal formation during scanning an even surface

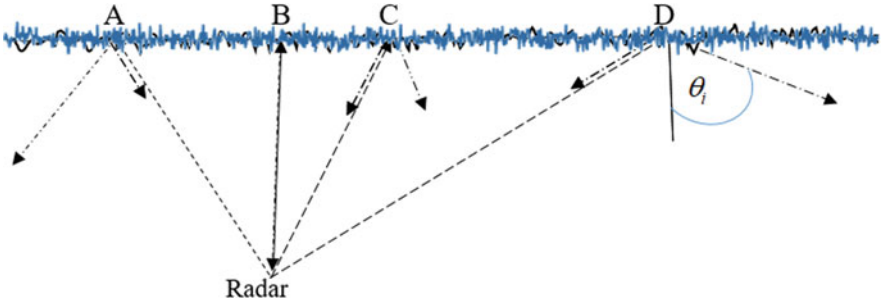

Fig. 6.2 The scheme of the echo signal formation from the even surface with small-scale irregularities

The scheme, shown in Fig. 6.2, is transformed into a scheme (Fig. 6.1) in cases where Rayleigh's criterion is fulfilled [6]

$$h < \frac{\lambda}{8 \cos \theta_i}, \tag{6.1}$$

where h is the largest height of small-scale surface roughness, λ is the wavelength of radiation, θ_i is the incidence angle of the wave on the surface at a certain point i (Fig. 6.2).

At point B, the incidence angle of the wave $\theta_i = 0$ and then $h < \frac{\lambda}{8}$. Hence, the EMW reflection at point B is a mirrored one if the maximum height of the surface irregularities does not exceed eighth of the wavelength. At $\lambda = 1$ m, this height reaches 12.5 cm, and from such an uneven surface, there is a mirror reflection. The domains around other points A, C, and D (usually this is the first Fresnel zone) form a diffuse reflection of the EMW in the direction toward the receiving radar antenna of the robot. For convenience and simplicity of the terminology, we will call the domain around point B, which reflects EMW in the direction of the radar antenna, a mirror point. If the Rayleigh criterion is not satisfied, the EMW reflection at point B is diffuse and the amplitude of the echo signal, as well as the probability of an amplitude jump, can be substantially reduced. Reflection of waves with small lengths from a flat surface, as a rule, is diffuse, since on a real surface, small-scale irregularities and vegetation exist almost always. Thus, in accordance with the Rayleigh criterion, it is necessary to use radiation with a relatively long wavelength $\lambda > 8h \cos \theta_i$ to obtain a mirror reflection of the EMW from a rough surface. For the conditions shown in Figs. 6.1 and 6.2, the mirror points from the domains A, C, and D cannot be obtained; however, if the earth or other surface is a curved one, then the appearance of echo signals from similar points becomes possible if $\theta_i = 0$, that is, the part of the curved surface is flat and perpendicular to the wave vector of the incident waves. Moreover, there may be several points B_1, B_2, and B_3, in which there is a mirror EMW reflection in the direction toward the radar antenna, which is installed on the mobile robot (Fig. 6.3).

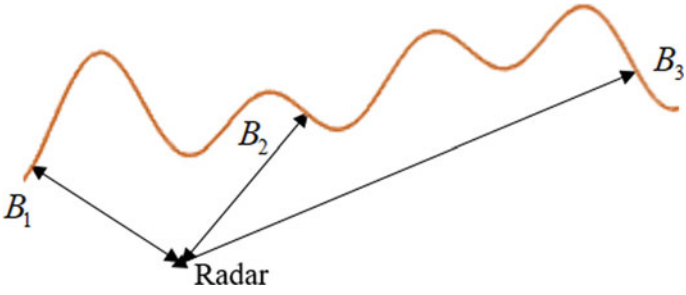

Fig. 6.3 The scheme of formation of echo signals from an uneven smooth surface

There are two main cases here. In the first case, the robot scans the surrounding space by antenna with a narrow antenna pattern (AP). This can be achieved using a small wavelength (centimeter or millimeter wavelength range). The irradiation of the points B_1, B_2, and B_3 is carried out sequentially, and the radar receiver takes the echo signal from each mirror point at different moments of time, and these points are distinguished by angular coordinates. In the second case, EMW with a large wavelength is used and the antenna has a wide AP.

EMW reflection from the points B_1, B_2, and B_3 becomes mirrored, but the echo signals are not distinguished by angular coordinates. In the antenna aperture, there is an interference electromagnetic field. By using this field, it is difficult to distinguish information about the reflected signal from each mirror point, the number of which may not be known. Determining the angular position in many cases needs a radar with a narrow AP antenna. Although the diffusive EMW scattering prevails, the mirror component of the signal's amplitude may be enough to distinguish a mirror point in the process of scanning against the background of diffuse reflection of the electromagnetic waves.

Previously, a heuristic analysis of the process of waves scattering from the earth's surface was carried out. There are various methods for calculating the characteristics of scattered waves, but it is impossible to use them in practice since it is difficult to describe the estimated situation because of changes in location conditions in the process of scanning and movement of the robot. However, during robot's navigation, it is expedient to get the maximum information about the surrounding area, especially when a priori information about the area is limited, for example, when a robot moves on another planet. The echo signals from the terrain contain information about the shape of the relief, the presence of vegetation, forests, and concentrated objects of artificial and natural origin. The characteristics of signals can be calculated in advance for the typical conditions of robot navigation using modern methods of analysis. Further, the intelligent systems that are installed at a robot will likely be able to determine the nature of the area on which it moves.

According to Rischka and Conrad [7], the landmark is a physical object created by man or nature, which is easily recognized by technical means. A landmark recognition by mobile robots involves the use of sequential comparison of the landmark video images with the reference images previously recognized [8]. Strict geometric methods of determining the landmark shape are not rational, since its real form can be blurred, for example, a pillar covered with trees, and the number of different landmarks can be large. In [7], it is reported that a database of 900 landmarks has been created. It is important here to determine the characteristic features of the landmark and to attribute it to any group, unless, of course, it is not unique. Consequently, there is a problem of constructing landmark models, as well as models of unknown terrain, which can be used to construct a map. The landmarks and unknown environmental models can be built not only based on video observations but also with radar observations, because in many cases it is difficult to obtain high-quality video images of landmarks and the surrounding terrain, for example, at night, fog, etc.

Currently, self-controlled robots have already been created. They can detect obstacles and automatically eliminate the possibility of collision with them. To do this, at a robot, ultrasound and other sensors are used together with the corresponding software [9]. The range of these sensors is small, and, therefore, they are compact and consume insignificant energy. Increasing the range of sensors is not required, which is due to the low speed of robots. For high-speed robots, for example, automatic cars, the requirements for the range of obstacles are increasing. A reliable means of implementing these requirements is the use of radars at robots.

A more powerful means of obtaining reliable and qualitative information about the surrounding space is the association of measurement information obtained by different types of sensors, for example, ultrasonic, radar, and mechanical. This is the problem of collecting measurers or mixing information from sensors built on various physical principles [10]. Localization of mobile robots on the ground most often uses triangulation methods [11], which also use radiation in different wavelengths, in particular laser, based on dynamic triangulation [12] and neural network for improving 3D laser scanner measurements [13]. Naturally, for the analysis of radar information, it is necessary to know the reflection properties of the surrounding area.

6.3 EMW Reflection from the Surrounding Area in Different Frequency Ranges

There are many scientific papers in which methods of calculating the parameters of scattered waves from the objects are analyzed. Let us consider them briefly and make the main conclusions from the results of theoretical and experimental studies, which may be useful for the robots' navigation.

The method of calculating the characteristics of scattered waves should be chosen based on the frequency range of the EMW, the polarization of the waves, the shape and state of the reflection surface, and some other factors that are not considered here. To calculate the characteristics of scattered waves on a surface with small-scale irregularities, the method of small perturbations is used, and if the radius of curvature of the surface is considerably greater than the wavelength, Kirchhoff's approximation is preferred [6]. To determine the required characteristics, it is necessary to have information about the coefficients of reflection of the EMW from the surface, which, in turn, depend on the complex dielectric permittivity $\dot{\varepsilon} = \varepsilon - j60\lambda\sigma$ of the surface, where ε is the real value of the dielectric permittivity of the soil, λ is the wavelength, and σ is the specific conductivity of the soil. For different types of soil, they are presented in Table 6.1 [14].

Table 6.1 presents the electrical characteristics of some homogeneous soils. In the presence of heterogeneous distributed objects on the ground, the electrical characteristics of a complex system are replaced by equivalent or effective values. If there is a vegetative cover on the black earth surface, then the effective value of the permittivity for the wavelength $\lambda = 3.2$ cm is $\varepsilon_{ef} = 4$–9.5 in summer and $\varepsilon_{ef} = 12$ in

Table 6.1 The values of components of the complex permittivity for different types of soils

No.	Kind of soil	The values of the components of dielectric permittivity	
		The real part of dielectric permittivity, ε	Specific conductivity of the soil σ, $\frac{\text{Cm}}{\text{m}}$
1	Snow	1.2	$2 \cdot 10^{-4}$
2	Dry soil	2.5–4	10^{-2}–10^{-1}
3	Wet soil	4–20	10^{-2}–3
4	Crystalline rocks	5–10	10^{-6}–10^{-4}
5	Water	60	10^{-3}–10
6	Seawater	80	4–6.6

winter. Similar characteristics at the same wavelength for meadows with shrubs are $\varepsilon_{\text{ef}} = 10$–12 in summer and $\varepsilon_{\text{ef}} = 2.3$–2.7 in winter, and for forest areas $\varepsilon_{\text{ef}} = 2.5$–5 at wavelengths from 1.25 to 70 cm. The specific conductivity of soil with abundant vegetation is very difficult to simulate, as many factors are affected on it.

From the given data, the electrical characteristics of the soil are diverse, and therefore, it is difficult to create a single model. As a result, after applying Maxwell's equations, we usually pass to the estimation of the fields of scattered waves, using the transport equation, the Green's functions, and approximate solutions of integral equations for the surface current [14]. The electromagnetic field of waves reflected from an arbitrary surface is determined as the sum of the field reflected from some average smooth surface (not necessarily equal), and the perturbation fields caused by the scattering of waves by small-scale irregularities. The boundary conditions are transferred from the general surface to an averaging smooth surface, which is a complicated procedure. Thus, in determining the general scattered field, the method of small perturbations and the Kirchhoff method are used simultaneously.

The concepts of small-scale and large-scale irregularities are closely related to the wavelength, as can be seen from the Rayleigh criterion. The surface shape, which is determined by a certain complex function $h(x, y)$, can be represented as the sum of the products of orthogonal functions on random coefficients, for example, coefficients of the Fourier series. For each type of surface, the random coefficients are distributed according to some law. For practical purposes, a function that describes the shape of a surface is often represented as the sum of three functions [15]. The first function describes large-scale irregularities, the second one small-scale, and the third one the effective height of the structure, which is formed by elements of vegetation. For navigation of robots, the reflection of the waves from the surface toward the radar antenna requires information on the reflection coefficient of the EMW in this direction. The surface in this case is modeled in the form of a set of facets, each of which is covered by small-scale irregularities [15]. The resulting field is the sum of the coherent and incoherent representations of all facets. The main factor determining the wave field is the phase relationship between the partial reflected waves, especially when the number of these waves is small.

The specific effective EMW reflection surface (scattering surface) of statistically rough isotropic surfaces at angles of falling close to zero (the wave vector

perpendicular to the plane tangent to the surface at a given point) is determined by the expression [15]

$$\sigma_0 = K_{f_0}^2 \frac{l_h^2}{4\sigma_h^2} e^{-\frac{l_h^2}{4\sigma_h^2} tg^2\theta}, \tag{6.2}$$

where K_{f_0} is the complex coefficient of the mirror reflection of EMW with frequency f_0, σ_h^2 is the variance of heights of small-scale irregularities, l_h is the radius of correlation of these irregularities, θ is the incidence angle of the wave to the surface (it is known that $\theta = 0$, if the waves reflect in the direction of the radar antenna).

The analysis of scattered waves by different structures of the surface has shown [15] that σ_0 depends on a complicated way on the frequency of the EMW. At large-scale irregularities of the surface, the specific reflection area is practically independent of frequency. Since the scale of irregularities substantially exceeds the wavelength, the mirror reflection of the waves dominates. It is the reason that with the increase of the angle of incidence of the wave on the surface, the part of mirror reflection toward radar and σ_0 sharply decreases rapidly. The presence of small-scale irregularities causes the change in the specific effective surface of the scattering, depending on the frequency of the laws from λ^0 to λ^{-4}. Thus, the radar of a robot can distinguish the presence of type of irregularities on the surface if it is equipped with transmitters and receivers operating at different frequencies. After calibration of the radar equipment, the reflected signals at different frequencies will be close in amplitude, if the waves reflect from mirror points, and on the surface, there are large-scale irregularities of the relief. During the robot movement, the nature of the terrain and the amplitude of the echo signals can vary, which is due to a significant dependence σ_0 on the presence of distributed objects on the surface. Table 6.2 describes some specific effective areas of wave reflection from the surface of the earth for different wavelengths [15].

Table 6.2 Specific effective areas of wave reflection from the earth's surface

No.	Type of terrain	Parameter values	
		Wavelength, λ, cm	Specific effective area, σ_0
1	Dense forest	3.2	0.1–0.8 (in summer)0.6–0.7 (in winter)
2	Woodland	0.86	0.08
		1.25	0.02–0.05
		3.3	0.003–0.06
3	Forest	8	0.8
		70	0.6
4	Meadow with shrubs	3.2	3–7 (in summer)
5	Inhomogeneous terrain	0.32	0.4
		0.86	0.9
6	Desert	8	2.2
		70	0.5

Thus, on the basis of the frequency dependence of the amplitudes of echo signals from the surface type, the nature of the roughness on it can be determined (large-scale and small-scale). More information on irregularities based on this approach is difficult to obtain. If during the scanning the domains of the surface are heterogeneous, then the analysis of the echo signals can lead to erroneous conclusions about the change of the irregularity's nature, whereas really the type of the terrain has changed. For example, the specific area of scattering at a wavelength of 0.86 cm is an order of magnitude smaller for wooded area than for inhomogeneous terrain without forest [15]. There are some important features for the practice of reflecting millimeter waves from the surface, which are considered, for example, in [16]).

In the optical range, waves dissipate diffusely from objects which are important for robot's navigation. The energy of the reflected waves is directly proportional to the diffuse scattering coefficient ρ_d, that is, to the ratio of the reflected and falling light flux [17].

In most cases, the lower values ρ_d correspond to smaller wavelengths of the optical range, and the upper values to the largest lengths of this range. Reflection from coniferous trees does not have such dependence. So, in the range $\lambda = 0.6$–0.7 μm with increasing wavelength, the coefficient ρ_d first decreases, and then increases again.

The summarized information of this section can be used to construct models of random processes of echo signal amplitudes that arise during the scanning of surface by a radar antenna of a robot.

6.4 Mathematical Models of Random Processes Describing the Amplitudes of Echo Signals from the Distributed Objects

Random processes of amplitude of echo signals at the input of the radar receiver are formed during scanning the surrounding space by an antenna of the radar while a robot moves. Even for a static robot, a random process is created after the radar antenna irradiates a certain part of the surface of distributed and concentrated objects. During scanning, the type of the surface is changed randomly for the observer due to changes in the relief, vegetation, and so on. Correspondingly, the characteristics of random echo signals are changed at the input and output of the radar receiver.

The size of the irradiated part of the surface depends on the width of the radar AP and distance between the robot and surface (Fig. 6.4). Reflected signals come to the antenna from all irradiated areas of the surface. Their amplitude is determined by the width of the AP and the type of the surface with small-scale irregularities and vegetation. With uniformly distributed characteristics of irregularities and vegetation, there is a certain stationary random process (Fig. 6.5) of amplitudes of echo signals at the receiver input. The wider the AP, the more reflective elements of the irradiated surface are involved into the echo signal creation in a certain direction, which leads

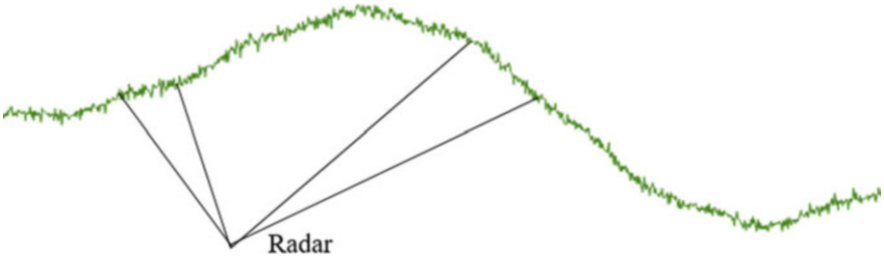

Fig. 6.4 A scheme of rough surface area irradiation by radar antenna with narrow antenna pattern

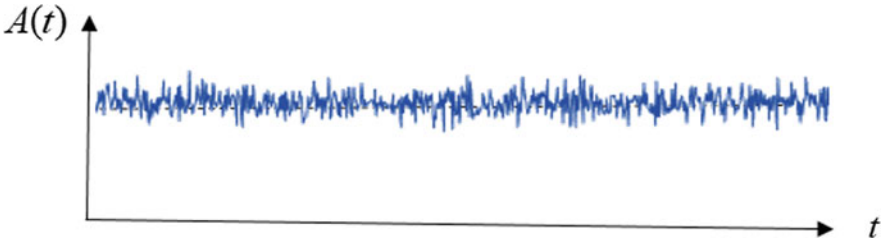

Fig. 6.5 An example of the realization of a stationary random process of amplitudes of echo signals that reflect from the rough surface during its scanning

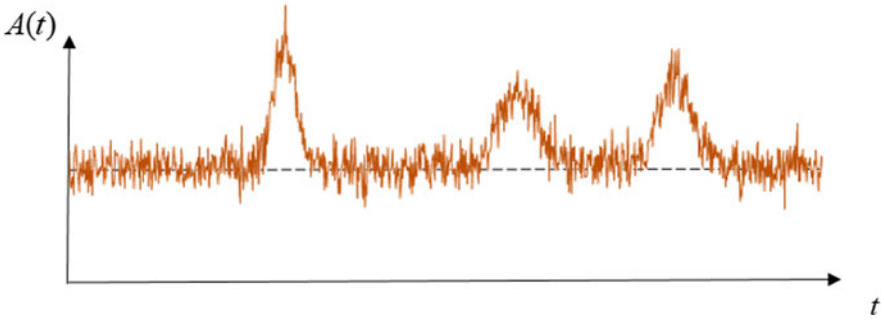

Fig. 6.6 An example of the realization of a random process of amplitudes of echo signals reflected from the rough surface during its scanning in the presence of mirror points on the surface

to the averaging of the amplitudes and a decrease of variance of the echo signal fluctuations. If the terrain changes radically, for example, there is a transition from the steppe to the wooded area, the variance of the echo signals can be substantially changed. This is an important feature for binding the robot to landmarks in navigation of the robots.

The process described above refers to the diffuse reflection of signals from the surface. In the presence of mirror points on the surface at certain moments of time due to the mirror component, the amplitude of the echo signal from the surface in a certain direction may increase sharply, that is, a jump of amplitude (Fig. 6.6) occurs.

This phenomenon can also be used for robot navigation. The amplitude of the jump is completely determined by the mirror component of the reflected signal, and the latter depends on the type of the surrounding area. The duration of the jump is determined by the scanning speed of space by the antenna. The shape of amplitude jump in simulation can be described by the Gaussian law. For reliable detection of a jump, it must have good energy characteristics, that is, amplitude and duration. The duration of the jump is determined by the nature of the transition from the completely diffuse reflection of the EMW from the surface to the mixed diffuse-mirror reflection and, naturally, the speed of space scanning. With a fast scan, the amplitude jump is difficult to detect against the background of diffuse reflected signals and interference. Slow scanning allows us to create conditions for detecting a amplitude jump.

Thus, in the scanning sector of an antenna with a narrow AP, the random process is represented by the sum of the stationary random process and random functions that at random moments describe the jumps of the amplitudes (Fig. 6.7).

If the length of the EMW is large (decimeter, meter waves), that is, the condition of mirror reflection (6.1) is executed, diffusely reflected echo signals will have a small amplitude in comparison with mirror signal amplitude, and in some cases,

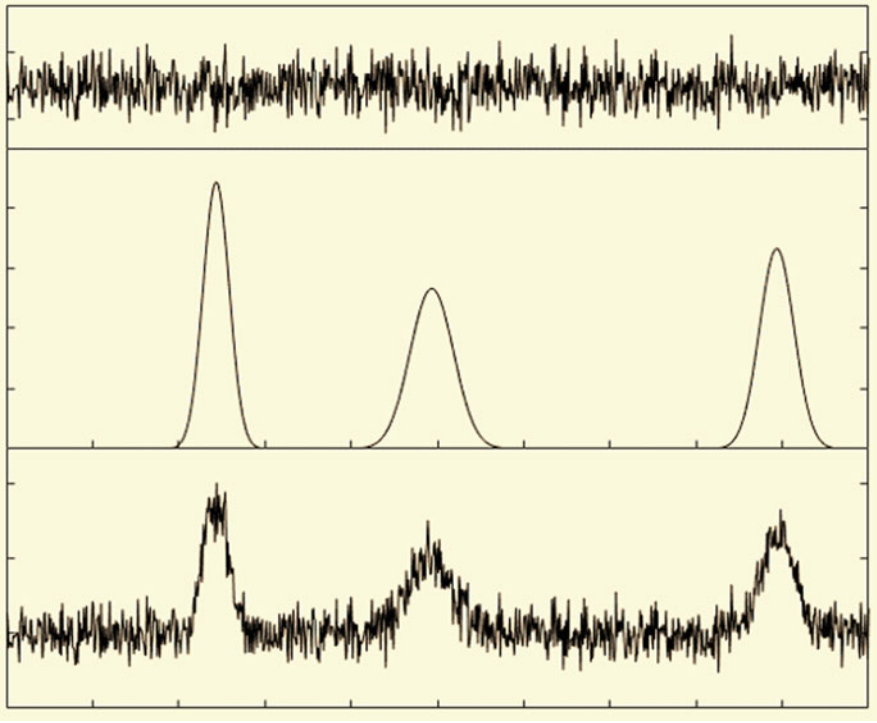

Fig. 6.7 A scheme of formation of a total random process of amplitudes of echo signals, reflected from a rough surface during its scanning, in the presence of three mirror points on the surface

they can be ignored. The radar AP at a robot of small size cannot be narrow, since its width is proportional to the wavelength and inversely proportional to the linear antenna size. Consequently, the antenna irradiates a large area of the surface. The echo signals from the surface are formed in the direction of the radar only from the mirror points. The number of these points is determined by the width of the AP and the type of large-scale irregularities on the surface, which, in general, determine its shape. For a flat surface, one should expect one mirror point. For a complex form surface, the number of mirror points can reach several units. If the mirror point is one, then diffuse signals are observed at the receiver input, the amplitude of which depends on the roughness, and on a large amplitude jump that can be easily found. In the presence of two mirror points, an interference pattern of two oscillations with different phases is formed, that is, the total oscillation may have amplitudes from zero to double amplitude from two mirror points. In this case, in the process of scanning within the width of AP, we can first get one mirror point, then two, then again one mirror point. Other variants of forming a total echo signal are possible. A similar picture is observed for cases of falling several mirror points into the width of the AP. A random process describing the echo signal from a rough surface in this case may be nonstationary. It can have a significant change in the mean value, but variance can behave in a complicated way: on the one hand, due to small diffuse scattering, it should be small, and on the other hand, due to random interference effects with deep fading, it can reach large values.

There is another option of EMW reflection from the surface when the number of mirror points is zero. This corresponds to the situation (Fig. 6.8) of scanning an oblique surface, when at the input of the receiver only diffuse reflected signals will be present. This is another feature of surface recognition by a radar of robot, but it is possible only with the use of large wavelengths in relation to the size of surface roughness.

Note that the characteristics of such waves are not distorted in the troposphere of the earth, that is, the influence of the medium on the propagation of radio waves can be neglected. Otherwise, it occurs with optical, millimeter, and even centimeter EMW, which are distorted in the troposphere due to the influence of precipitation,

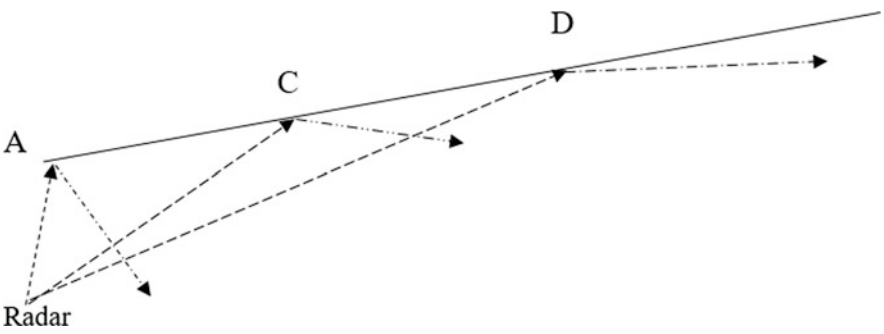

Fig. 6.8 Illustration of the absence of mirror points on an irradiated flat surface

fog, gases, etc. We will assume that the range of the location is relatively small, so that at distances such distortions of the characteristics of the echo signals do not reach large values, that is, they should not be considered.

Now let us consider the effective surface area of distributed and concentrated (point) objects, that is, backscatter echo area of these objects. The radar of a robot irradiates the surrounding area in angular range, which is determined by the angles θ, φ in two orthogonal planes. The transmitter power is P, transmitter antenna gain is $G = G_{\text{m}}F^2(\theta, \varphi)$, where G_{m} is the maximum antenna gain and $F^2(\theta, \varphi)$ is the normalized antenna pattern. The receiving antenna has the maximum value of the effective aperture area $A_{\text{ef}_{\text{m}}}$.

Using [18], one can obtain the formula for the radar cross section (RCS) σ_e of a diffusely scattering surface when it irradiates by EMW along the normal. At an angle θ from the normal, we have

$$\sigma_e(\theta) = 4S_e R_{h,v}\cos^2\theta, \tag{6.3}$$

where irradiated area on the scattering surface on the range r within the width of the AP in two orthogonal planes $2\theta_{0.5\text{P}}$ and $2\varphi_{0.5\text{P}}$

$$S_e \approx r^2 \cdot 2\theta_{0.5\text{P}} \cdot 2\varphi_{0.5\text{P}} \tag{6.4}$$

The coefficients of EMW reflection from the surface $R_{h,\,v}$ are the effective coefficients, that is, they consider the presence of vegetation on the surface, etc. If the maximum value of the effective aperture area of the receiving antenna is $A_{\text{ef}_{\text{m}}}$, the signal power at the receiver output

$$P_r = \frac{PG_{\text{m}}A_{\text{ef}_{\text{m}}}F^4(\theta, \varphi)\, R_{h,v}2\theta_{0.5\text{P}}2\varphi_{0.5\text{P}}\cos\theta}{(4\pi r)^2}. \tag{6.5}$$

We consider that the domain of the surrounding area is simultaneously irradiated by two antennas at different frequencies with the same width of the antenna. It is easy to pick up by selecting the size of the antennas and the amplitude–phase distribution of the electromagnetic field in their aperture. Before use, the measuring channels at both frequencies are calibrated by changing the parameters P, G_{m}, $A_{\text{ef}_{\text{m}}}$ during irradiation of an even conductive surface from the same range. The result of the calibration is the uniformity of the amplitudes of the reflected signals in both frequency channels from the direction of the main lobes of the APs.

Let us consider the following model situation. The robot scans the surrounding area at two different frequencies that are significantly different. Let, for example, the wavelength of horizontal polarization in the first frequency channel does not exceed 3 cm, and the second frequency channel is in the meter range. As a result of scanning a flat surface by EMW at two frequencies, the time dependences of the amplitude realization of the reflected signal at the input of a radar receiver are shown in Fig. 6.9.

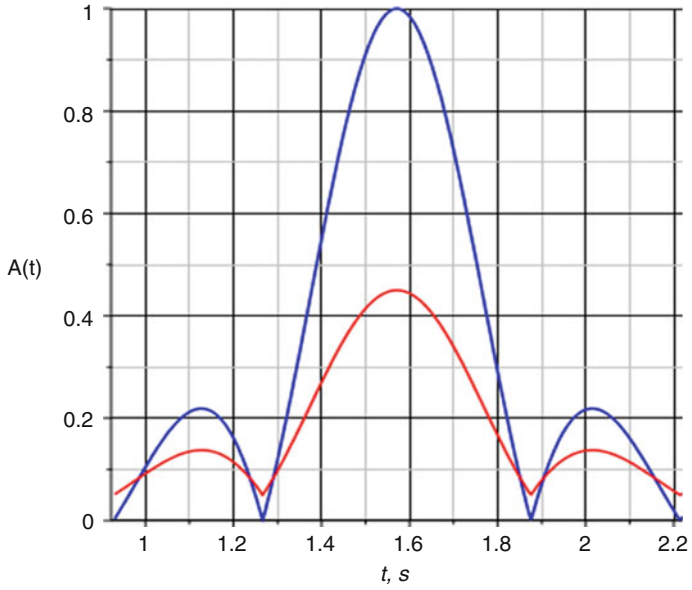

Fig. 6.9 The examples of the time dependences of the normalized amplitudes of signals, reflected from the even rough surface: the red line shows the amplitude of the signal in the first frequency channel; blue, in the second one

The time dependence of the amplitudes completely repeats the form of APs, and in the meter range (second channel), the field amplitude is greater than that in the first one, since the module of the coefficient of EMW reflection from the soil in the meter range is higher than that in the centimeter one. When the soil moisture increases, the difference between the red and the blue curves in the amplitude decreases. Because of the diffuse scattering of the centimeter EMW, the zero amplitude values in the first frequency channel (red line) disappear and the amplitude falls in the direction of the main maximum of the AP. Thus, the presence of small-scale roughness on a surface can be recognized qualitatively by the presented feature.

In the presence of mirror points on the surface, the above dependence $A(t)$ is destroyed (Fig. 6.10). In the meter range, the condition for mirror reflection of the EMW (Rayleigh criterion) is still preserved, and therefore, in some directions, there arise interference extrema of the field. In the centimeter band of the EMW, the dependence of the total field on time is complex and differs essentially from the previously deduced dependencies (Fig. 6.10).

It is easy to see that the reflection of an EMW from an uneven rough surface forms the complicated structure of electromagnetic field at both frequencies. This kind of dependence is exactly the evidence of a substantially uneven surface. Here, however, it should be noted that if the correlation radius of large-scale irregularities is significantly greater than the value $r \cdot 2\theta_{0.5\mathrm{P}}$ or $r \cdot 2\varphi_{0.5\mathrm{P}}$, for example, in Fig.

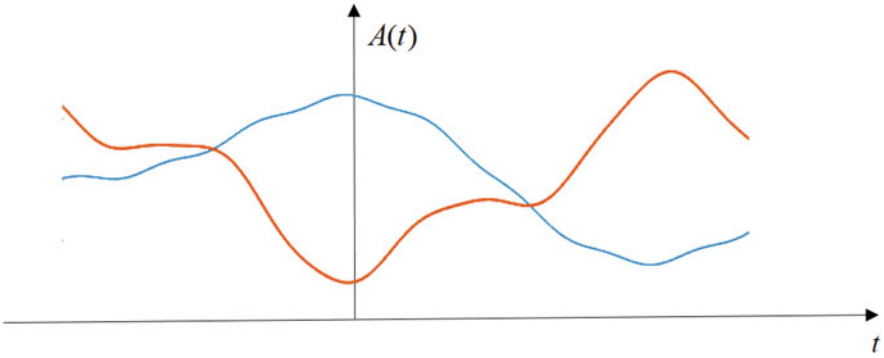

Fig. 6.10 The examples of the time dependences of the signal amplitudes reflected from the rough surface with three mirror points: the brown signal shows the amplitude of the signal in the first frequency channel; blue, in the second one

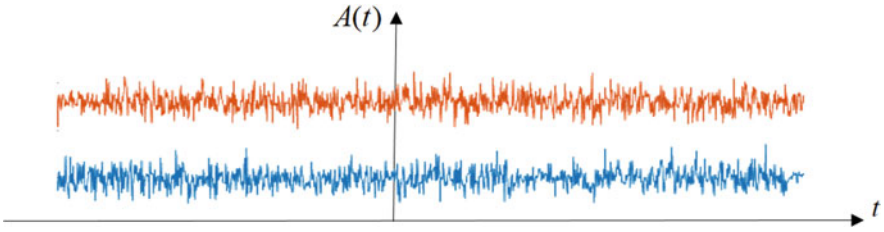

Fig. 6.11 The examples of the time dependences of the signal amplitudes reflected from the rough surface: the red signal shows the amplitude of the signal in the first frequency channel; blue, in the second frequency

6.4, this case is similar to the previous situations, since the number of mirror points tends to one.

In practice, the situation is often encountered, as shown in Fig. 6.8. In this case, the EMW of meter band almost does not reflect in the direction of the radar if the Rayleigh criterion is fulfilled. On the contrary, the centimeter EMW diffusely scatter in the direction of the radar, as shown in Fig. 6.11.

The analysis of the figures shows that the comparison of the amplitudes of the signals of two frequencies reflected from the surface allows to estimate approximately the type of terrain of the surrounding area. The obtained results form a priori information for the robots about the environment.

Until now, the time dependences of the amplitudes of signals reflected from the terrain during the process of its scanning were considered. Echo signals can also be obtained without scanning the environment. In this case, the antenna of a robot is stationary, and the maximum of the AP is directed perpendicular to the line of the robot's motion. As a result, it should be expected that dependencies (Fig. 6.9) would be converted into other ones similar to Fig. 6.5.

Consequently, the presence on the ground of concentrated objects, which can serve as landmarks for autonomous mobile robots, challenges the detection of such objects and their coordinates with respect to other landmarks. Immobility of most landmarks prevents the use of Doppler methods for separating echo signals from landmarks in the presence of signals that are reflected from stationary terrain. The only approach is to develop methods for detecting abrupt changes in the energy characteristics of echo signals from the terrain that arise during scanning the surrounding area or moving the robot along this area with fixed antenna. If the landmark is located on the background of a complicated relief of the terrain, then scanning the terrain will indeed lead to sharp changes in the amplitude of the echo signals ("jumps") as under the influence of interference effects in the adding of signals, reflected from the mirror points and as a result of appearance of concentrated objects within the irradiated region that can be used as landmarks. Reliable detection of amplitude jump signals in this case is impossible. However, for the case presented in Fig. 6.10, the level of the reflected signals from the terrain in both frequency channels is significantly reduced. Thus, the most convenient situation in which the possibility of detecting ground landmarks is possible is the location in the direction of the sloping terrain, which has little forest and shrubs. This case can be considered as the main one for navigating the robots. Hence, it is necessary to estimate the radar cross section of concentrated objects and decide whether their choice can be used as landmarks.

Let us divide conditionally all practical situations into two groups. The first group includes all cases in which a significant part of the energy of EMW from the reflecting surface is directed to the antenna radar of a robot (e.g., Figs. 6.1 and 6.2). The second group covers cases of only diffuse reflection of EMW from the surface (e.g., Fig. 6.8). The simplest mathematical model of the complex amplitude of reflected monochromatic signals is

$$\dot{A}(t) = \sum_{k=1}^{m} \dot{A}_k(t) e^{j\varphi_k(t)} + n(t) \tag{6.6}$$

where $\dot{A}_k(t)$, $\varphi_k(t)$ are respectively random complex amplitudes and phases of the echo signals, reflected from the kth mirror point at the input of the radar receiver, m is the random number of such mirrored points, $n(t)$ is the white noise.

The model (6.3) describes the amplitude of the reflected signals in the first group. In the second group, there is a sum of many diffuse components with low energetic characteristics. For physical reasons, reliable detection of abrupt changes in the amplitude of echo signals is possible only in the second group. For a numerical estimation of this possibility, it is necessary to know the model of the echo signals from the landmark as a concentrated object.

6.5 Mathematical Models of Random Processes Describing Amplitudes of Echo Signals from Concentrated Objects

The different concentrated objects of natural and artificial origin with various scattering properties can be used as a landmark. Sometimes they are called the point objects, because their size is much smaller than the size of distributed objects.

The radar cross section (RCS) of concentrated objects is given, for example, in [19]. Therefore, RCS of a ball with perfectly conducting surface and radius $r \gg \lambda$ is

$$\sigma = \pi r^2 \tag{6.7}$$

The RCS of a circular cylindrical metal pillar with radius r and length L is determined by the formula [20]

$$\sigma_{\max} = \frac{2\pi r L^2}{\lambda} \tag{6.8}$$

RCS of a metal rectangular plate with dimensions a and b, which is much larger wavelength, is

$$\sigma_{\text{p}} = \frac{4\pi S^2}{\lambda^2} \tag{6.9}$$

where S is the area of the plate, the largest size of which is significantly smaller than the distance r between the robot and the plate. The formula (6.9) is given for the direction of the radar—the domain of the surface.

The analysis of formulas (6.7)–(6.9) shows that the RCS of the concentrated objects varies depending on the wavelength of the EMW. This may be the basis for the previous robot recognition of the landmark type. However, the main task is to recognize the situation that is peculiar for the first and second group of reflected signals. As previously indicated, this can be done on the basis of the use of essential differences in random processes describing echo signals at different frequencies that are significantly different. The robot's decision about existence of the second group in the given time range leads to the need for analysis of echo signals from useful objects, that is, landmarks. It turns out that the RCS of these objects in the centimeter range exceeds a similar index in the meter range, as can be seen from the formulas (6.4)–(6.9). For the signals of the first group, everything was the opposite. Consequently, this feature of RCS can be used to identify a situation that is characteristic of the first group.

The dependence of the RCS of the concentrated objects on the angular coordinates most often takes the form of a type $\frac{\sin\alpha}{\alpha}$, that is, it has a main lobe and several side lobes. To detect the amplitude jumps of the echo signals, only the main lobe has the actual value. Note that the AP of the radar also has a similar shape. Then the angle α can be represented as a product $\Omega \cdot t$, where Ω is an angular scanning speed of the

antenna. That is why the amplitude of the echo signal from the landmark should be approximated by the Gaussian dependence

$$A(t) = \frac{A_0}{\sigma_\alpha \sqrt{2\pi}} e^{-\frac{(\Omega \cdot t)^2}{2\sigma_\alpha^2}} \tag{6.10}$$

where A_0 is some amplitude of the reflected signal, chosen during the simulation or determined in the process of experimental research, and σ_α is a parameter characterizing the width of the Gaussian dependence. It should also be considered that $\alpha \leq \alpha_{\max}$, where $\alpha_{\max}$ is the maximum value of the angle within which the radiation and the reception of echo signals occur.

Hence, the maximum jump of the amplitude of the echo signal is proportional to the maximum RCS value $\sigma_{\max}$ and is frequency dependent. In the first and second frequency channels of the receiver, the statistical characteristics of the echo signals from the environment should be described by white noise, the level of which in the centimeter range will most often be higher than in the meter range. The ratio of amplitude jumps of the echo signals from the cylindrical metal pillar in the first and second frequency channels are evaluated by the receiver measuring system and estimated by the formula

$$\frac{\Delta A_1}{\Delta A_2} \approx \frac{f_1}{f_2} \tag{6.11}$$

where f_1 and f_2 are the frequency of signals in the first and second frequency channels, respectively. If the landmark is a flat rectangular plate, the ratio of the amplitudes of these echo signals in both frequency channels is

$$\frac{\Delta A_1}{\Delta A_2} \approx \left(\frac{f_1}{f_2}\right)^2 \tag{6.12}$$

which follows from a formula like (6.11) [20].

The described method makes it possible not only to recognize the landmarks in some cases but also to find a connection of the MAR coordinates with these landmarks. If the robot's trajectory lies not far from the landmarks L_1 and L_2 (Fig. 6.12), then at the points S_1 and S_2 at different times the robot can detect these landmarks. Since the distance d between these points and the angles β_{ij} are known in advance, the distance to the landmarks at each point of the robot's trajectory is determined by the methods of triangulation. Here the index i shows the number of the current position on the trajectory of the robot, and the index j is the landmark number.

Assume that the error of determining the distance d between the current points of the robot's trajectory is small. Then, the precision of estimating the position of the robot relative to the landmark is determined by the errors of measuring the angle coordinates β_{ij}. As a result, the spatial errors of the determination of the working

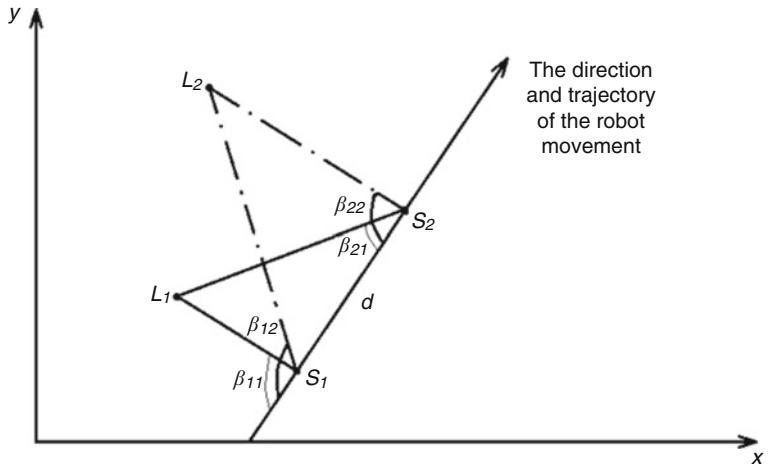

Fig. 6.12 Trajectory of the robot's motion relative to two landmarks

robot's position will be distributed within the ellipse with the axes $k\sigma_\xi$ and $k\sigma_\eta$ [21], where $k = \sqrt{-2\ln(1-p_0)}$ and p_0 is a probability of getting the robot's position errors into the ellipse with the indicated axes. The coefficient $k = 2.15$ for $p_0 = 0.90$ and $k = 3$ for $p_0 = 0.99$. The dimension of the error ellipse for one landmark is estimated by the formulas [21]

$$\sigma_\xi = \left(\sum_{i=1}^{2} \frac{\cos^2 \beta_i}{\rho_i^2 \sigma_i^2} \right)^{-0.5} \tag{6.13}$$

$$\sigma_\eta = \left(\sum_{i=1}^{2} \frac{\sin^2 \beta_i}{\rho_i^2 \sigma_i^2} \right)^{-0.5} \tag{6.14}$$

where ρ_i is the distance from the robot's antenna (point S_1 or S_2) to the landmark, σ_i^2 is the variance of the errors of angle coordinate determination by the robot antenna.

The spatial errors σ_ξ, σ_η of robot's positions essentially depend on the distance ρ_i between the robot and the landmark and are reduced at short distances. If, at a distance $\rho_i \approx 300$ m, the landmark orientation is determined with errors not exceeding 10 m, then the measurement error of the angular coordinate is about 1°, which is not a problem for the radio engineering system of the robot.

The use of two frequency channels or channels with the processing of fundamentally different signals (microwave, ultrasound, laser, etc.) provides the mutual processing of measurement information that is hidden in the echo signals. The development of optimal systems for measuring the echo signal parameters and

the object coordinates useful for the robots is a very important problem, but usually the classical schemes perceive the signal amplitude jumps as interfering spikes and smooth them out.

6.6 Measurement of Amplitude Jump of Signals for Landmark Detection by Mobile Autonomous Robots

Since the signal reflected from the landmark often has no peculiarities compared to the background signal, its reliable detection by traditional methods is practically impossible. However, there are opportunities to detect some landmarks. During scanning the surrounding space by an antenna of the robot, a random process of the amplitude of echo signal from the area irradiated by the transmitter is observed at the input of the on-board receiver. The realizations of this process contain fluctuation components, the nature of which is due to the conditions of EMW reflection from the background elements of the terrain. The reflected signal from a landmark may be hidden in these fluctuations, unless there is a resonance scattering of the EMW from this landmark. In this case, during the terrain scanning, a amplitude jump may occur that exceeds the background reflection of the waves and the internal and external noise acting on the receiver input. The duration of the jump depends on the speed of the scanning. The jump of the echo signal amplitude can also occur if, in a short time, the nature of the area on which the robot moves essentially changes. The section deals with the method of detecting jumps of the echo signals, which allows, in some cases, to use this jump to identify a possible landmark by a mobile robot.

Detailed approaches to detecting abrupt changes in the dynamical system occurring in unknown moments of time are set out in [1] (abrupt changes at an unknown time point). In order to determine the abrupt (sharp) changes in [1], a unified approach is proposed within the general statistical theory of quality control, signal processing, automatic signal segmentation, and navigation monitoring systems. It is based on the use of the likelihood ratio algorithm and estimation of the statistical properties of the system. Before and after an abrupt change, two major models of the stochastic process are analyzed, and Kullbek's information is determined. To detect abrupt changes, a non-parametric Bayesian approach is used. The value of the signal parameter after the change is considered as known, and the probabilistic characteristics of this change are not evaluated.

In the general case, obtaining an estimation of the signal parameter is carried out by observing the maximum of the conditional a posteriori probability density of the parameter described, for example, by the Fokker–Planck–Kolmogorov equation. This stochastic equation in partial derivatives describes the evolution of the conditional a posteriori probability density for the Markov process. It is very complex and cannot be solved analytically [22]. A similar equation for high-frequency signals was obtained by [23]. Maltsev and Silaev [24, 25] developed optimal algorithms for evaluating the state of a dynamic system and identifying random jump-like

variations of its parameters and determining the moments of their occurrence. The systems of differential equations for a posteriori density of the probabilities of the parameters of random processes, the solution of which by the approximate methods leads to obtaining current estimates of parameters in a real time scale and the median estimation of the jump moment, are obtained. The analysis is carried out for the system described by the autoregressive process with a correlation coefficient jump at a random moment of time. In [26], an optimal system for detecting and estimating the sharp changes (jumps) of the amplitude of vibrations of machines in real time was developed. The main aspects of this approach to detecting landmarks for mobile robots are published in [27–29].

According to [1], the change in the signal parameter can be considered as abrupt change if it occurs almost instantaneously or less than the sampling period, which for MAR depends on the antenna rotational speed. The robot's antenna scans the terrain in a wide range of angles. The angular size of a landmark is small, and the time of its radiation by this antenna is also little. This indicates that the signal reflected from the landmark exists for a short time interval, that is, it generates a signal with a sharp amplitude change, which we call the jump. The form of the amplitude jump is like the shape of the antenna pattern, and, in the simulation, it will be represented by a Gaussian impulse reflected from a metal pillar, for example. The electromagnetic wave will be observed against the background of echo signals from the environment. Their amplitude in time is described by some random processes. For simulation, we will use reference random processes that characterize the reflection properties of a certain terrain and are described by known stochastic differential equations (SDRs), for example, of the following type:

$$\frac{dA(t)}{dt} = -\alpha \cdot t + n(t), \tag{6.15}$$

$$\frac{dA(t)}{dt} = a\,(A, t) + b\,(A, t) \cdot n(t). \tag{6.16}$$

In these equations, the parameter α characterizes the correlation properties and the spectrum width of the random process, $n(t)$ is a white noise, and the functions $a(A, t)$, $b(A, t)$ are used to form a nonstationary random process. All functions must be selected so that the random process is like the behavior of the reflected signals from the terrain.

The amplitude of the reflected signals from the terrain depends on many factors, for example, transmitter power and receiver sensitivity, antenna characteristics, range to reflecting elements of the terrain, effective surface of the scattering of objects in the area, etc. In order not to deal with a wide range of amplitudes of echo signals, we will normalize the obtained amplitude values to unity and accordingly simulate jumps of different intensity, duration, which occur at random moments of time at different levels of noise $n(t)$. The jumps should not significantly exceed the echo

signal background. The time scale should be consistent with the speed of scanning the surrounding area. A various number of jumps can be used to conduct the study.

The usual optimal system of signal amplitude measurement is not capable of qualitatively estimating rapid sudden changes of amplitudes (jumps of amplitudes). It is necessary to synthesize an optimal system that considers the peculiarities of the jumps of amplitudes in an unknown (in advance) instant of time. Such a system is based on the Fokker–Planck differential equation. Derivation of the system of stochastic differential equations for estimating amplitudes of jumps and their variances is presented in [27], and the final result is described by Eqs. (6.17)–(6.20).

$$\frac{dp_1}{dt} = P_{\tau_{\text{jump}}}(t) \cdot e^{-z} + \frac{1}{N} \cdot p_1 \cdot (1 - p_1) \left\{ \begin{array}{l} A \cdot \Delta A_1 \left[1 - \cos\left(\varphi_0 - \varphi_1\right)\right] + \frac{1}{2}\left(A_1^2\right) - \\ - \sigma^2_{\Delta A_1} + 2 \cdot n(t) \cdot \Delta A_1 \cdot \sin\left(\omega \cdot t + \varphi_1\right) \end{array} \right\} \tag{6.17}$$

$$\frac{dz}{dt} = \frac{p_1}{N} \left\{ \begin{array}{l} A \cdot \Delta A_1 \left[1 - \cos\left(\varphi_0 - \varphi_1\right)\right] + \\ + \frac{1}{2}\left(\Delta A_1^2 A - \sigma^2_{\Delta A_1}\right) + 2 \cdot n(t) \cdot (A_1) \cdot \sin\left(\omega \cdot t + \varphi_1\right) \end{array} \right\} \tag{6.18}$$

$$\frac{d\Delta A_1}{dt} = \frac{1}{p_1} \cdot P_{\tau_{\text{jump}}}(t) \cdot e^{-z} \cdot (\Delta A_0 - \Delta A_1) + V_1(t) \cdot \frac{1}{N} \cdot \left[2 \cdot y(t) \cdot \sin\left(\omega \cdot t + \varphi_1\right) - A \cdot \cos\left(\varphi_0 - \varphi_1\right) - \Delta A_1\right] \tag{6.19}$$

$$\frac{dV_1}{dt} = \frac{1}{p_1} \cdot P_{\tau_{\text{jump}}}(t) \cdot e^{-z} \cdot \left[(\Delta A_0 - \Delta A_1)^2 + V_0 - V_1\right] - \frac{1}{N} \cdot V_1^2 \tag{6.20}$$

where

p_1—a posteriori probability of detecting the signal amplitude jump
z—relative speed operation of the system
ΔA_0, ΔA_1—a priori and a posteriori amplitude jump estimations
$V_1(t)$—variance of a posteriori amplitude jump distribution
$V_0(t)$ —variance of a priori amplitude jump distribution
t—time
τ_{jump}—the moment of the signal amplitude jump from the value $A_0(\tau_{\text{jump}})$ to another value $A_1(\tau_{\text{jump}})$
$\varphi_0(t)$, $\varphi_1(t)$—the phase of the signal before and after the jump, respectively
$n(t)$—white Gaussian noise with zero mean and spectral intensity N

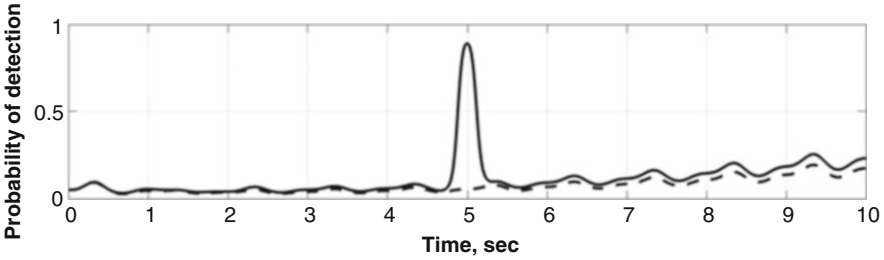

Fig. 6.13 The probability of detecting the amplitude jump for the random process when the amplitude jump is absent (dotted line) and if it exists (solid line)

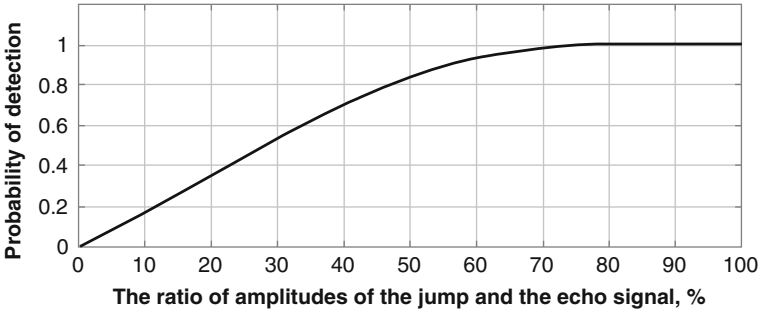

Fig. 6.14 The probability of detecting a jump of amplitude from the ratio of the amplitude of this jump to the mean amplitude of the echo signals from the terrain

The solution of the system of differential Eqs. (6.17)–(6.20) under the corresponding initial conditions allows to obtain the important characteristics of the landmarks detection system. The dependence of the probability of detecting the amplitude of the signal jump from time is shown in Fig. 6.13. If the jump is absent, then the probability is close to zero (Fig. 6.13, dotted line), and if it really exists, this probability for this example is closer to 1 (Fig. 6.13, solid line).

The probability of amplitude jump detection essentially depends on the energy characteristics of the jump, that is, its amplitude and duration. Figure 6.14 describes the dependence of this probability on the amplitude jump of constant duration. For the conditions given earlier, the probability 0.8 is achieved even when the amplitude jump exceeds half the mean amplitude of the signal that is reflected from the terrain (Fig. 6.14).

The estimation of the amplitude jump obtained as a result of the solution of the system of Eqs. (6.17)–(6.20) is presented in Fig. 6.15. The system is not able to determine the jump shape, but the value of this jump determines well.

The accuracy of estimating the jump of the amplitude is determined from the variance equation (fourth Eq. 6.20) of the system (6.17)–(6.20). The time dependence of the variance is shown in Fig. 6.16.

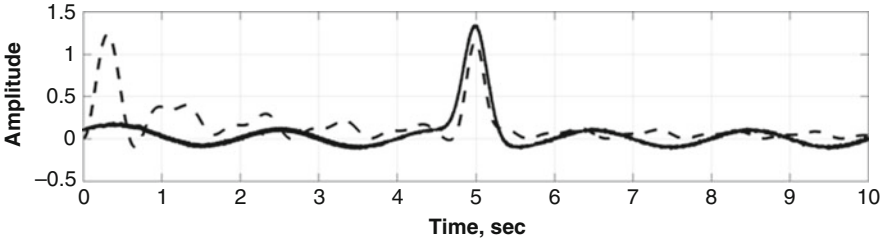

Fig. 6.15 The realization of random process with amplitude jump (solid line) and result of its estimate (dotted line)

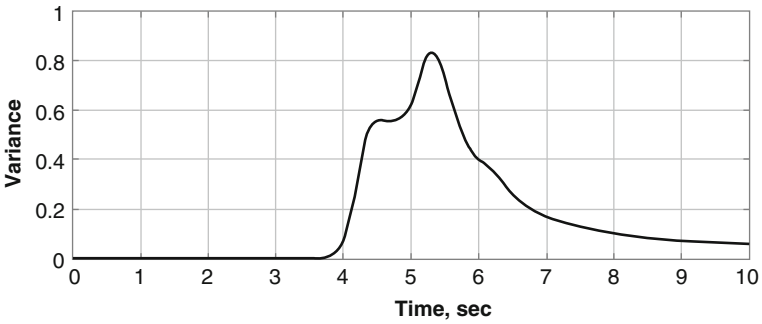

Fig. 6.16 An example of the time dependence of the amplitude jump variance

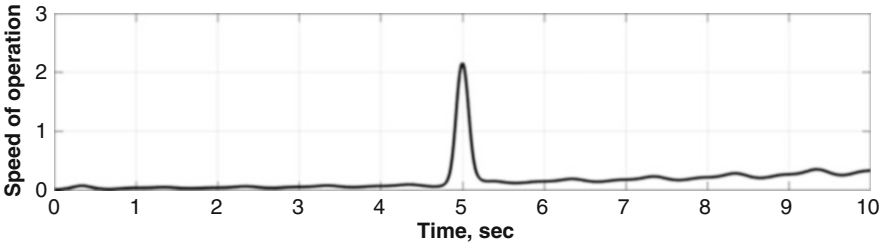

Fig. 6.17 An example of time dependence of operation system rate

Only after a while the variance of the amplitude jump decreases to small values. This time depends on the operating speed of the system, which is determined from the second equation of the system (6.17)–(6.20) and is shown in Fig. 6.17.

So, determining the amplitude jump takes some time which is not critical for relatively slow MAR. The results of the simulation are obtained for the case of the absence of a priori information about the time of an amplitude jump occurrence, which means that the given numerical results characterize the worst properties of the system of detection and evaluation of amplitude jumps of echo signals from landmarks. The presence of any information about jumps increases the quality of their detection and extends the scope of the method. For example, the navigation

systems described in [1, 4] can provide a priori information about the robot's position, which increases the probability of detecting landmarks and increases the accuracy of the estimation of the amplitudes of jumps and the accuracy of the coordinate measurement of the robot.

It should be emphasized that the detection of amplitude jumps of echo signals from landmarks is based on the evaluation of energy characteristics, regardless of the physical nature of such jumps. That is why it is possible to detect noise surges that are similar to jumps in signal amplitudes and, as a result, to reduce the probability of correct identification of landmarks. Hence, the requirements for the reliabilities of detected jump parameters, which differ significantly from the parameters of noise surges, increase.

The developed approach to detecting jumps of the echo signal amplitude is based on the use of the Fokker–Planck–Kolmogorov equations that have a wide application. For example, we have developed a similar method for detecting sudden changes in economic processes [27].

References

1. Colle, E., & Galerne, S. (2017). A multihypothesis set approach for mobile robot localization using heterogeneous measurements provided by the internet of things. *Robotics and Autonomous Systems, 96*, 102–113. Elsevier.
2. Garulli, A., & Vicino, A. (2001). Set membership localization of mobile robots via angle measurements. *IEEE Transactions on Robotics and Automation, 17*(4), 450–463.
3. Lindner, L., Sergiyenko, O., Rivas-Lopez, V., Hernandez-Babluena, D., Flores-Fuentes, W., Rodríguez-Quiñonez, J. C., Murrieta-Rico, F. N., Ivanov, M., Tyrsa, V., & Basaca, L. C. (2017). Exact laser beam positioning for measurement of vegetation vitality. *Industrial Robot, 44*(4), 532–541.
4. Sergiyenko, O. Y. (2010). Optoelectronic system for mobile robot navigation. *Optoelectronics, Instrumentation and Data Processing, 46*(5), 414–428.
5. Prorok, A., Gonon, L., & Martinoli, A. (2012). Online model estimation of ultra-wideband TDOA measurements for mobile robot localization. In *IEEE International Conference on Robotics and Automation (ICRA)* (8 p). Saint Paul, USA.
6. Ishimaru, A. (1978). *Wave propagation and scattering in random media. Vol. 2: Multiple scattering, turbulence, rough surfaces and remote sensing* (317 p). New York: Academic.
7. Rischka, M., & Conrad, S. (2014). Landmark recognition: State-of-the-art methods in a large-scale scenario. In *Proceedings of the 16th LWA Workshops: KDML, IR and FGWM* (pp. 10–17). Aachen, Germany.
8. Schmid, C., & Mohr, R. (1996). Combining greyvalue invariants with local constraints for object recognition. In *Proceedings of the Conference on Computer Vision and Pattern Recognition* (pp. 872–877). San Francisco, CA, USA.
9. Hanumante, V., Roy, S., & Maity, S. (2013). Low cost obstacle avoidance robot. *International Journal of Soft Computing and Engineering (IJSCE), 3*(4), 52–55.
10. Kandylakis, Z., Karantzalos, K., Doulamis, A., & Karagiannidis L. (2017). Multimodal data fusion for effective surveillance of critical infrastructure. In *Frontiers in spectral imaging and 3D technologies for geospatial solutions*, 25–27 October 2017 (pp. 87–93). Jyväskylä, Finland.
11. Borenstein, J., Everett, H. R., Feng, L., & Wehe, D. (1997). Mobile robot positioning- sensors and techniques. *Journal of Robotic Systems, 14*(4), 231–249.

12. Real-Moreno, O., Rodriguez-Quiñonez, J. C., Sergiyenko, O., Basaca-Preciado, L. C., Hemandez-Balbuena, D., Rivas-Lopez, M., & Flores-Fuentes, W. (2017). Accuracy improvement in 3D laser scanner based on dynamic triangulation for autonomous navigation system. In *Industrial Electronics (ISIE). 2017 IEEE 26th International Symposium on IEEE* (pp. 1602–1608).
13. Rodriguez-Quiñonez, J. C., Sergiyenko, O., Basaca-Preciado, L. C., Hemandez-Balbuena, D., Rivas-Lopez, M., Flores-Fuentes, W., & Basaca-Preciado, L. C. (2014). Improve 3D laser scanner measurements accuracy using a FFBP neural network with Widrow-Hoff weight/bias learning function. *Opto-Electronics Review, 22*(4), 224–235.
14. Krasiuk, N. P., Koblov, V. L., & Krasiuk, V. N. (1988). Influence of the troposphere and underlying surface on radar. In *Radio and communication* (216 p). (in Russian).
15. Zubkovich, S. G. (1968). Statistical characteristics of radio signals reflected from the earth's surface. In *Sov radio* (224 p). (in Russian).
16. Kulemin, G. P., & Razskazovsky, V. B. (1987). The scattering of millimeter radio waves by the earth at low angles. *(Scientific thought)* (232 p). (in Russian).
17. Lukianov, D. P., et al. (1981). Laser measuring system. In *Radio and communication* (456 p). (in Russian).
18. Skolnik, M. I. (1990). *Radar handbook* (846 p). New York: McGraw-Hill.
19. Grishin, J. P., Ignatov, V. D., Kazarinov, J. M., & Ulianitskiy, J. A. (1990). Radio engineering systems. In *High school* (496 p). (in Russian).
20. Rajyalakshmi, P., & Raju, G. S. N. (2011). Characteristics of radar cross section with different objects. *International Journal of Electronics and Communication Engineering, 4*(2), 205–216.
21. Shirman, J. D. (1970). Theoretical foundation of radar. *Sov radio* (560 p). (in Russian).
22. Sharma, S. N. (2008). A Kolmogorov-Fokker-Planck approach for a stochastic Duffing-van der pol system. *Differential Equations and Dynamical Systems, 16*, 351–377.
23. Stratonovich, R. L. (1968). *Conditional Markov process and their application to the theory of optimal control* (367 p). Amsterdam: Elsevier.
24. Maltsev, A. A., & Silaev, A. V. (1985). Detection of jump-shaped parameter changes and optimal estimation of the state of discrete dynamic systems. *Automation and Telemechanic*, 45–58. in Russian.
25. Maltsev, A. A., & Silaev, A. V. (1989). Optimal estimation of moments of random jump changes of signal parameters. *Radio Engineering and Electronics, 34*(5), 1023–1033. in Russian.
26. Poliarus, O. V., Barchan, V. V., Poliakov, Y. O., & Koval, A. O. (2009). The optimal system for detecting and estimating the jumps of amplitudes of dynamic objects vibrations. *East European Journal of Advanced Technology, 6/6*(42), 21–23. (in Ukrainian).
27. Poliarus, O. V., Poliakov, Y. O., Nazarenko, I. L., Borovyk, Y. T., & Kondratiuk, M. V. (2018). Detection of jumps parameters in economic processes (on the example of modelling profitability). *International Journal of Engineering & Technology, 7*(4.3), 488–496.
28. Poliarus, O. V., Poliakov, Y. O., & Lindner, L. (2018). Determination of landmarks by mobile robot's vision system based on detecting abrupt changes of echo signals. In *Proceedings of the 44th Annual Conference of the IEEE Industrial Electronics Society* (pp. 3165–3170). Washington, DC, USA.
29. Poliarus, O., Poliakov, Y., Sergiyenko, O., Tyrsa, V., Hernandez, W., & Nechitailo, Y. (2019). Azimuth estimation of landmarks by mobile autonomous robots using one scanning antenna. In *Proceedings of IEEE 28th International Symposium on Industrial Electronics* (pp. 1682–1687). Vancouver, BC, Canada.